

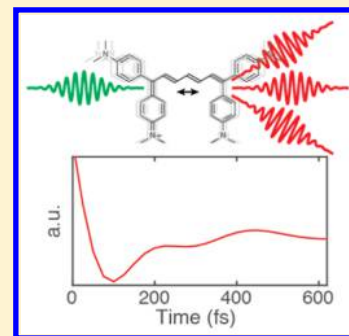
Isolated Ground-State Vibrational Coherence Measured by Fifth-Order Single-Shot Two-Dimensional Electronic Spectroscopy

William O. Hutson, Austin P. Spencer, and Elad Harel*

Department of Chemistry, Northwestern University, 2145 Sheridan Road, Evanston, Illinois 60208, United States

S Supporting Information

ABSTRACT: Vibrations play a critical role in many photochemical and photophysical processes in which excitations reside on the electronically excited state. However, difficulty in assigning signals from spectroscopic measurements uniquely to a specific electronic state, ground or otherwise, has exposed limitations to their physical interpretation. Here, we demonstrate the selective excitation of vibrational coherences on the ground electronic state through impulsive Raman scattering, whose weak fifth-order signal is resonantly enhanced by coupling to strong electronic transitions. The six-wave mixing signals measured using this technique are free of lower-order cascades and represent correlations between zero-quantum vibrational coherences in the ground state and single-quantum coherences between the ground and electronic states. We believe that this technique has the potential to shed much-needed insight onto some of the mysteries regarding the origin of long-lived coherences observed in photosynthetic and other coupled chromophore systems.



In recent years, there has been tremendous effort to try to understand the basic physical mechanism behind highly efficient energy transfer in biological and bioinspired systems.^{1–3} Sophisticated nonlinear optical techniques, most notably coherent two-dimensional (2D) spectroscopy,^{4–6} performed on numerous systems have revealed long-lived oscillatory signals, whose origins are still topics of contentious debate.^{7,8} Whether these signals originate in the ground or excited electronic states reflects different physical interpretations of the role of coherence in energy transfer. For instance, vibrations that couple strongly to electronic transitions, (i.e., vibronic excitons) give rise to long-lived oscillatory signals according to several theoretical calculations.^{9,10} Unfortunately, underdamped vibrations in the ground electronic state also yield nearly identical signals, while these nuclear motions do not have a straightforward influence on energy transfer that resides in the excited-state manifold.¹¹ One of the key limitations is that third-order 2D experiments, which utilize a series of three resonant optical pulses to induce time-dependent polarization in the sample, have difficulty distinguishing between ground- and excited-state coherences, especially in circumstances in which the nonadiabatic contributions to the state character are substantial.¹² In this Letter, we introduce a new fifth-order method that utilizes both resonant and nonresonant optical excitations to uncover previously unobserved correlations between low-frequency molecular motions and specific electronic excitations. We discuss the advantages of using nonresonant excitations to select specific signal pathways, which simplifies the interpretation of coherent beating signals.

In 2D Fourier transform (2DFT) spectroscopy and other four-wave mixing (4WM) methods,¹³ a series of three ultrafast pulses induces polarization in the sample, which acts as a source for a fourth emitted electric field, as depicted in the energy ladder diagram in Figure 1A. When the time delays between the

pulses are systematically sampled, correlations between different optical transitions, assigned to the excitation axis, ω_v , and rephasing axis, ω_b , for each waiting time, T , are encoded into the signal, $S^{(3)}(\omega_v, T, \omega_b)$.^{14–16} Notably, 2DFT spectroscopy has made significant contributions toward understanding a variety of photoinduced physical processes: energy transfer in photosynthetic protein complexes,^{17–19} interactions between electronic and vibrational degrees of freedom in heterodimers,²⁰ and correlating the motion of electrons to strong Coulombic coupling in GaAs quantum wells,²¹ just to name a few.

There are many signal generation pathways induced by the 2DFT spectroscopy pulse sequence,²² but we will focus primarily on pathways in which a single- or zero-quantum coherence evolves within the interpulse delay periods. In Figure 1A, the first resonant excitation creates a coherence between the ground and electronic excited state of the system, which evolves for a time interval, τ , (i.e., single-quantum coherence), as seen in the Feynman diagram describing the 4WM process in Figure 1B. The second resonant excitation may potentially create any of the following time-dependent processes: (i) a vibrational wavepacket localized on the ground state, (ii) a vibrational wavepacket localized on the excited state, (iii) an electronic coherence between the excited states, or (iv) a vibronic coherence in which the electronic and vibrational coordinates strongly couple.¹⁴ After time interval T , the final resonant excitation returns the system to a single-quantum coherence, and then the signal radiates during the time interval t . The phase of the emitted field, therefore, is the sum of the

Received: August 3, 2016

Accepted: August 30, 2016

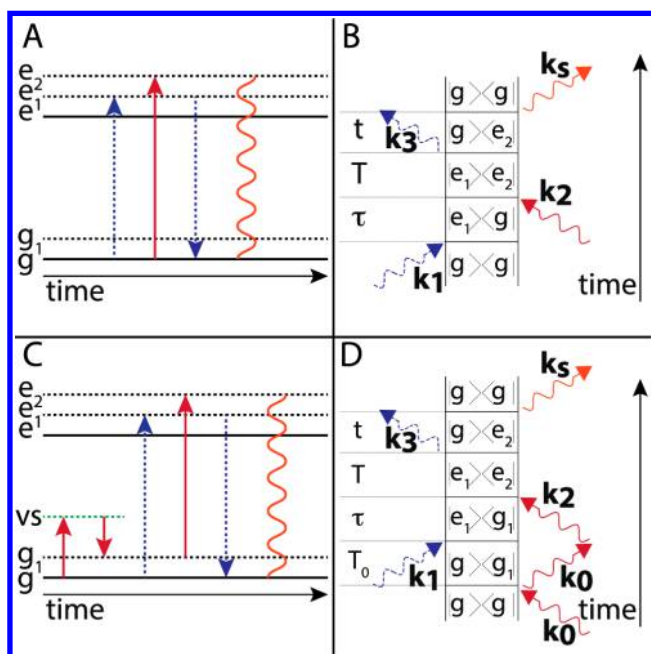


Figure 1. Energy ladder and Feynman diagrams for one particular 4WM (A,B) and 6WM (C,D) pathway. k_i defines the wave vector for the i th pulse (subscript s denotes the signal). g_i and e_i are ground and electronic states, respectively, on the i th vibrational state. vs is a “virtual state” involved in the impulsive Raman scattering process. For all diagrams, dashed blue arrows correspond to operating on the ket and solid red arrows correspond to operating on the bra.

phase accumulated during each interpulse delay period.²³ The signal amplitude during T will show a combination of decay and oscillatory behavior depending on the specific pathways involved. Unfortunately, the origin of the oscillatory signal, a coherence of the types (i)–(iv), is generally difficult, if not impossible, to definitively assign.^{12,24,25}

To overcome this limitation, we have employed electronically off-resonant (EOR) excitation. EOR excitations have been used in some Raman spectroscopic techniques and have the potential to excite vibrational transitions that originate from

specific electronic states.²⁶ Ernsting et al. used femtosecond-stimulated Raman spectroscopy (FSRS) with an actinic pulse to produce a $\chi^{(5)}$ signal that selectively probes vibrational coherences on the excited state of β -carotene.²⁷ However, a notable drawback of FSRS is that it is inherently a mixed time–frequency technique. The Raman pump pulse, which is spectrally narrow and temporally broad, may interact with the system at any point during the pulse envelope, which both mixes and creates new pathways in the detected signal.²⁸ It is therefore critical to enforce strict time-ordering in order to restrict rather than increase the number of pathways, which makes interpretation of the signals far more tractable.

Here, we incorporate an EOR pulse into a single-shot 2DFT method called gradient-assisted photon echo spectroscopy (GRAPES; see the Supporting Information).^{29,30} The EOR pulse initiates a vibrational wavepacket on the ground electronic state before subsequent resonant excitations are applied. The EOR pulse is slightly red-shifted ($\lambda_{\text{EOR}} > \lambda_{\text{GRAPES}}$) from the subsequent resonant excitations and is therefore preresonant (rather than fully nonresonant) with the ground-to-excited-state transition, as indicated by the first two interactions in the energy ladder diagram shown in Figure 1C. The preresonant condition is important as it allows sufficient coupling to the excited state to enhance impulsive Raman scattering processes while inhibiting excitation of appreciable excited-state population. The time delay between the preresonant pulse and the GRAPES pulse sequence, T_0 , acts as an additional Fourier dimension in the experiment, as labeled in the Feynman diagram in Figure 1D. As the initial Raman process introduces two additional light–matter interactions, the radiated signal corresponds to a six-wave mixing (6WM) process. Another key feature of this 6WM technique is that the ground-state coherence is resonantly enhanced by coupling to strong electronic-transition dipole moments of the system. This enhancement is important because it magnifies the impulsive Raman scattering signal strength above that of other competing pathways that do not experience the same magnitude of resonant enhancement.

In order to demonstrate that indeed we observe ground-state vibrational coherences, we carried out 6WM experiments on

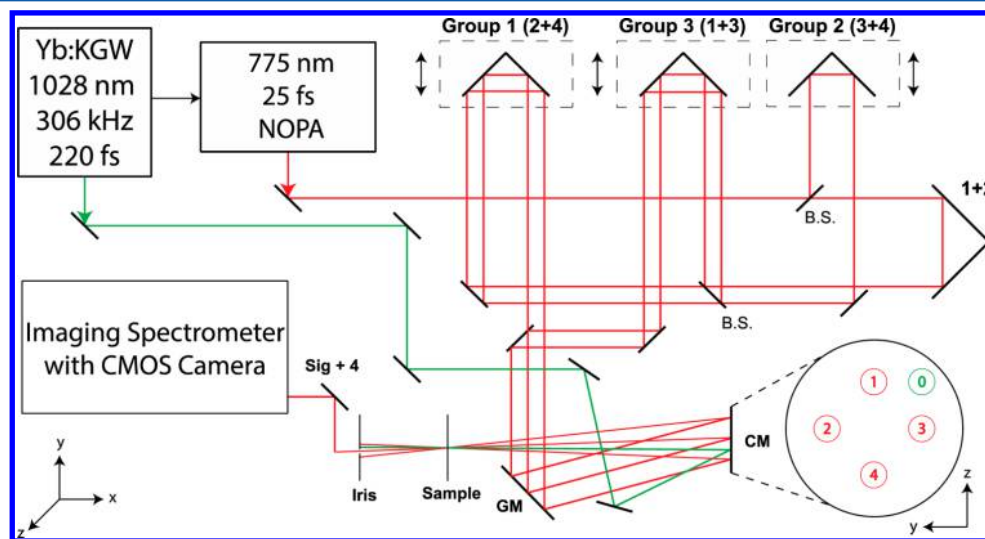


Figure 2. 6WM optical setup using a passively phase-stabilized geometry. Three motorized stages control the time delays between specific beam pairs. “1+2” is a fixed delay stage for pulses 1 and 2. Not shown are the choppers for beams 0 and 3. B.S. = beamsplitter, CM = cylindrical mirror (20 cm focal length), and GM = GRAPES mirror. The samples were flowed through a 200 μm path length quartz cell.

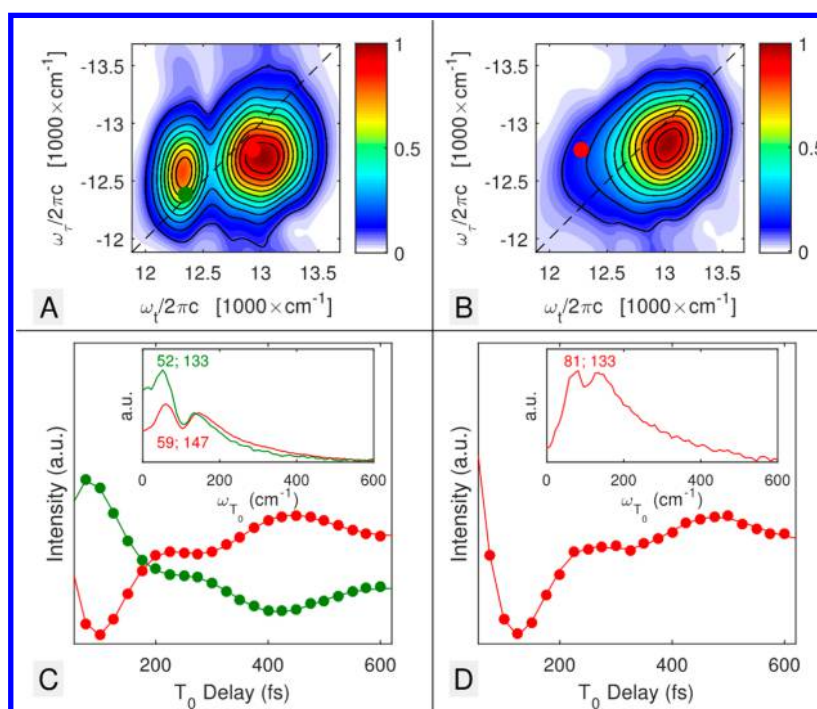


Figure 3. Absolute value 2DFT spectra of IR-895 and IR-140 6WM signals [A,B, respectively]. Real T_0 transients for IR-895 and IR-140 [C,D, respectively; insets: FFT of the real T_0 transients]. Each transient and FFT is color coded to denote from which position on the 2DFT spectrum the transient was derived (see the main text). The red and green numbers adjacent to the FFT's represent the frequencies extracted from the FFT of the respective T_0 transient in cm^{-1} .

two related cyanine molecules: IR-895 and IR-140 dissolved in methanol. These near-IR dyes were selected because their absorbance spectra conveniently lie within the bandwidth of our laser pulse. Furthermore, IR-140 shows evidence of low-frequency ($<200 \text{ cm}^{-1}$) vibrational beats that can be initiated using our EOR laser pulse³¹ (see the [Supporting Information](#)), and IR-895, given its similar structure, is also expected to show low-frequency beats. GRAPES has been described in detail elsewhere;^{29,30} therefore, the discussion of the experimental setup will focus primarily on addition of the nonresonant pulse and detection of the 6WM signal (see [Figure 2](#) and the [Supporting Information](#)).

Four beams (pulses 1, 2, 3, and 4) are derived from the output of a tunable noncollinear optical parametric amplifier (NOPA), pumped by an amplified Yb laser system. The EOR pulse originates directly from the amplified laser system (1028 nm, ~ 220 fs) without further modification except for power attenuation. The setup is passively phase-stabilized by the judicious combination of two beamsplitters used to produce beams 1–4, similar to a scheme previously reported.³² Beams 1–4 are reflected off of retroreflectors on a set of three delay stages such that the temporal delays between pulses 0 and 1 (T_0) and pulses 2 and 3 (T) are precisely controlled. The beams, arranged in a BOXCAR geometry on a cylindrical mirror (focal length = 20 cm), interact with the sample, as previously described, and the 6WM signal, $S^{(5)}(T_0, \omega_p, T, \omega_i)$, is emitted from the sample and overlapped with beam 4 (local oscillator) in the phase-matched, but not background-free, direction, $k_{\text{sig}} = \pm k_0 \mp k_1 + k_2 + k_3$. The signal is reimaged from the sample to the slit of a spectrograph and detected with a camera. The 6WM signal is isolated from the collinear 4WM signal using a chopper subtraction scheme (see the [Supporting Information](#)). Both choppers and the camera are phase-locked to the laser pulse train, ensuring that each image collected is an

average of the same number of laser shots. Experiments were performed for all samples by setting T to a constant delay time (100 fs) and subsequently scanning T_0 over equal time steps of 25 fs from 0 fs to 2 ps. The signal was averaged to obtain adequate signal-to-noise (see the [Supporting Information](#)).

[Figure 3](#) shows the absolute value 2DFT spectra of the 6WM signal for IR-895 and IR-140, projected onto the (ω_p, ω_i) plane for $T_0 = 350$ fs and $T = 100$ fs, the real part of their respective T_0 transients with exponential fits subtracted out from 75 to 600 fs, and the fast Fourier transforms (FFTs) of those transients using their full temporal range (0 fs to 2 ps) (see the [Supporting Information](#) for the fitting procedure). The T_0 transients were derived from the following positions in the 2DFT spectra: IR-895 [Position A: $\omega_p = 12\,800 \text{ cm}^{-1}$, $\omega_i = 12\,929 \text{ cm}^{-1}$; Position B: $\omega_p = 12\,400 \text{ cm}^{-1}$, $\omega_i = 12\,351 \text{ cm}^{-1}$], and IR-140 [Position A: $\omega_p = 12\,800 \text{ cm}^{-1}$, $\omega_i = 12\,270 \text{ cm}^{-1}$].

The 2DFT spectra for both dyes show evidence of beats present in the T_0 scan. It is interesting to note that unlike 4WM 2DFT the beating frequencies observed are not necessarily connected to the cross-peak selected in the 2D spectrum. That is, the resonant pulse interaction may connect different states than those excited by the EOR pulse. Therefore, even points on the diagonal of the electronic fifth-order 2D spectrum may show beating T_0 transient signals. A beating frequency of about 133 cm^{-1} for IR-140 is observed at almost every point within the 2D electronic spectrum, which is close to the beating frequency of 121 cm^{-1} observed using transient absorption (TA) with 800 nm and 38 fs pulses.³¹ This discrepancy can be explained by noting that the temporally long (~ 220 fs) and spectrally narrow ($\sim 87 \text{ cm}^{-1}$) pulse used here convolves with the molecular response, resulting in amplified low-frequency oscillations and shifted frequency positions. Nonetheless, the T_0 transient and FFT for both samples show clear evidence of beating and close correspondence (to within $\sim 10 \text{ cm}^{-1}$) of the

low-frequency beat to TA measurements of molecular vibrations. Due to the resonant pump pulse used in TA, the observed vibrations cannot be definitively assigned to either the ground or electrically excited state as both frequencies are expected to be quite close. Due to the EOR pulse in our 6WM experiment, the vibrations reported here must originate from the ground state via an impulsive Raman scattering process.

A general advantage of this technique over a TA measurement is the ability to interrogate which electronic transitions are coupled to certain ground-state vibrations. By projecting $S^{(5)}(T_0, \omega_r, T, \omega_i)$ onto the (ω_r, ω_i) plane, a particular diagonal or cross-peak can be selected (i.e., a certain ω_r and ω_i combination can be selected), and the vibrations from ω_{T_0} can be extracted. In effect, scanning within the (ω_r, ω_i) plane determines which ground-state vibrations are likely associated with certain Feynman pathways. TA measurements would not be able to attain this resolution of pathway specificity, even in the case of spectrally resolved TA. This advantage of our 6WM method over simple TA experiments is significant for extending the use of this technique to other samples of interest (e.g., photo-synthetic complexes or coupled chromophores).

One concern for 6WM experiments is that low-order cascades, phase-matched consecutive 4WM signals resulting from distinct chromophores, may dominate the true 6WM signal from isolated chromophores.^{33,34} Our data indicate that the 6WM signal from the solute does not have any substantial contributions from solute cascades. This is supported by a linear, rather than quadratic, concentration dependence of the signal at low optical densities (OD < 0.2). As shown in Figure 4, the signal peaks at ~ 0.3 OD before dropping due to other

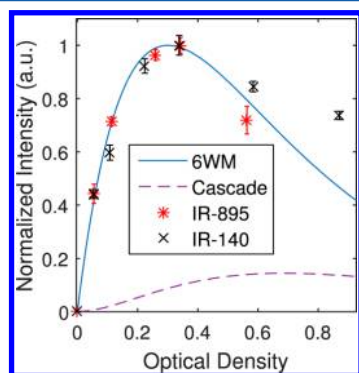


Figure 4. Experimental signal strength, propagation distortion theory, and cascade theory as a function of OD. For the experimental data and propagation distortion theory, the diagonal peak of 775 nm ($\sim 12\,900\text{ cm}^{-1}$) was selected. The experimental data are the result of performing all of the 6WM analysis and then recording the intensity at the $(\omega_r = 12\,900\text{ cm}^{-1}, \omega_i = 12\,900\text{ cm}^{-1})$ data point in the 6WM 2DFT spectrum at $T_0 = 0$ fs. The error bars were determined by taking the standard deviation of five 6WM measurements and dividing by the square root of the number of measurements. The cascade theory shows the proportion of cascades theoretically derived from the propagation distortion theory (see the Supporting Information for details).

effects (i.e., reabsorption). Further experiments were done to rule out 6WM signals from the solvent, as well as cascade signals from the solvent, solvent to solute, or solute to solvent. We conclude that the dominant (>94%) source of signal in these experiments is the 6WM signal from the cyanine dye (see the Supporting Information for detailed explanation).

In summary, we have demonstrated a method to measure ground-state-specific beating signals at each point in the 2D electronic spectrum. We measured low-frequency vibrational modes in a pair of related cyanine dyes, excited by EOR pulses and amplified by strong electronic transition dipole moments ($S_0 \rightarrow S_1$) of the system. Furthermore, we rigorously ruled out lower-order cascade signals that would otherwise contaminate the signal of interest. Future work will focus on correlating the vibrational coherence created by the EOR pulse with zero-quantum coherences created by resonant excitations. These experiments will inject much needed physical insight into the origin of quantum coherence in a wide variety of chemical systems.

EXPERIMENTAL METHODS

Supporting Information is available that provides detailed information regarding the experimental apparatus, sample preparations, cascade analysis, and T_0 transient fitting procedure.

ASSOCIATED CONTENT

Supporting Information

The Supporting Information is available free of charge on the ACS Publications website at DOI: 10.1021/acs.jpcllett.6b01733.

Detailed information regarding the experimental apparatus, sample preparations, cascade analysis, and T_0 transient fitting procedure (PDF)

AUTHOR INFORMATION

Corresponding Author

*E-mail: elharel@northwestern.edu.

Notes

The authors declare no competing financial interest.

ACKNOWLEDGMENTS

This work was supported by the Air Force Office of Scientific Research (FA9550-14-1-0005), and the Packard Foundation (2013-39272) in part.

REFERENCES

- (1) Caram, J. R.; Lewis, N. H. C.; Fidler, A. F.; Engel, G. S. Signatures of Correlated Excitonic Dynamics in Two-Dimensional Spectroscopy of the Fenna-Matthew-Olson Photosynthetic Complex. *J. Chem. Phys.* **2012**, *136*, 104505.
- (2) Halpin, A.; Johnson, P. J. M.; Tempelaar, R.; Murphy, R. S.; Knoester, J.; Jansen, T. L. C.; Miller, R. J. D. Two-Dimensional Spectroscopy of a Molecular Dimer Unveils the Effects of Vibronic Coupling on Exciton Coherences. *Nat. Chem.* **2014**, *6*, 196–201.
- (3) Harel, E.; Engel, G. S. Quantum Coherence Spectroscopy Reveals Complex Dynamics in Bacterial Light-Harvesting Complex 2 (LH2). *Proc. Natl. Acad. Sci. U. S. A.* **2012**, *109*, 706–711.
- (4) Turner, D. B.; Hassan, Y.; Scholes, G. D. Exciton Superposition States in CdSe Nanocrystals Measured Using Broadband Two-Dimensional Electronic Spectroscopy. *Nano Lett.* **2012**, *12*, 880–886.
- (5) Skoff, D. R.; Laaser, J. E.; Mukherjee, S. S.; Middleton, C. T.; Zanni, M. T. Simplified and Economical 2D IR Spectrometer Design Using a Dual Acousto-Optic Modulator. *Chem. Phys.* **2013**, *422*, 8–15.
- (6) West, B. A.; Moran, A. M. Two-Dimensional Electronic Spectroscopy in the Ultraviolet Wavelength Range. *J. Phys. Chem. Lett.* **2012**, *3*, 2575–2581.
- (7) Cheng, Y.-C.; Fleming, G. R. Dynamics of Light Harvesting in Photosynthesis. *Annu. Rev. Phys. Chem.* **2009**, *60*, 241–262.
- (8) Engel, G. S.; Calhoun, T. R.; Read, E. L.; Ahn, T.-K.; Mancal, T.; Cheng, Y.-C.; Blankenship, R. E.; Fleming, G. R. Evidence for

Wavelike Energy Transfer Through Quantum Coherence in Photosynthetic Systems. *Nature* **2007**, *446*, 782–786.

(9) Plenio, M. B.; Almeida, J.; Huelga, S. F. Origin of Long-Lived Oscillations in 2D-Spectra of a Quantum Vibronic Model: Electronic Versus Vibrational Coherence. *J. Chem. Phys.* **2013**, *139*, 235102.

(10) Chin, A. W.; Prior, J.; Rosenbach, R.; Caycedo-Soler, F.; Huelga, S. F.; Plenio, M. B. The Role of Non-Equilibrium Vibrational Structures in Electronic Coherence and Recoherence in Pigment-Protein Complexes. *Nat. Phys.* **2013**, *9*, 113–118.

(11) Monahan, D. M.; Whaley-Mayda, L.; Ishizaki, A.; Fleming, G. R. Influence of Weak Vibrational-Electronic Couplings on 2D Electronic Spectra and Inter-Site Coherence in Weakly Coupled Photosynthetic Complexes. *J. Chem. Phys.* **2015**, *143*, 065101.

(12) Tiwari, V.; Peters, W. K.; Jonas, D. M. Electronic Resonance with Anticorrelated Pigment Vibrations Drives Photosynthetic Energy Transfer Outside the Adiabatic Framework. *Proc. Natl. Acad. Sci. U. S. A.* **2013**, *110*, 1203–1208.

(13) Mukamel, S. Multidimensional Femtosecond Correlation Spectroscopies of Electronic and Vibrational Excitations. *Annu. Rev. Phys. Chem.* **2000**, *51*, 691–729.

(14) Jonas, D. M. Two-Dimensional Femtosecond Spectroscopy. *Annu. Rev. Phys. Chem.* **2003**, *54*, 425–463.

(15) Mukamel, S. *Principles of Nonlinear Optical Spectroscopy*; Oxford University Press: New York, 1995.

(16) Cho, M. *Two-Dimensional Optical Spectroscopy*; CRC Press: Boca Raton, FL, 2009.

(17) Panitchayangkoon, G.; Hayes, D.; Fransted, K. A.; Caram, J. R.; Harel, E.; Wen, J.; Blankenship, R. E.; Engel, G. S. Long-Lived Quantum Coherence in Photosynthetic Complexes at Physiological Temperature. *Proc. Natl. Acad. Sci. U. S. A.* **2010**, *107*, 12766–12770.

(18) Ostroumov, E. E.; Mulvaney, R. M.; Cogdell, R. J.; Scholes, G. D. Broadband 2D Electronic Spectroscopy Reveals a Carotenoid Dark State in Purple Bacteria. *Science* **2013**, *340*, 52–56.

(19) Brixner, T.; Stenger, J.; Vaswani, H. M.; Cho, M.; Blankenship, R. E.; Fleming, G. R. Two-Dimensional Spectroscopy of Electronic Couplings in Photosynthesis. *Nature* **2005**, *434*, 625–628.

(20) Hayes, D.; Griffin, G. B.; Engel, G. S. Engineering Coherence Among Excited States in Synthetic Heterodimer Systems. *Science* **2013**, *340*, 1431–1434.

(21) Stone, K. W.; Gundogdu, K.; Turner, D. B.; Li, X.; Cundiff, S. T.; Nelson, K. A. Two-Quantum 2D FT Electronic Spectroscopy of Biexcitons in GaAs Quantum Wells. *Science* **2009**, *324*, 1169–1173.

(22) Wright, J. C. Multiresonant Coherent Multidimensional Spectroscopy. *Annu. Rev. Phys. Chem.* **2011**, *62*, 209–230.

(23) Hybl, J. D.; Albrecht Ferro, A.; Jonas, D. M. Two-dimensional Fourier Transform Electronic Spectroscopy. *J. Chem. Phys.* **2001**, *115*, 6606–6622.

(24) Albert, J.; Falge, M.; Gomez, S.; Sola, I. R.; Hildenbrand, H.; Engel, V. Communication: Vibrational and Vibronic Coherences in the Two Dimensional Spectroscopy of Coupled Electron-Nuclear Motion. *J. Chem. Phys.* **2015**, *143*, 041102.

(25) Butkus, V.; Zigmantas, D.; Valkunas, L.; Abramavicius, D. Vibrational vs. Electronic Coherences in 2D Spectrum of Molecular Systems. *Chem. Phys. Lett.* **2012**, *545*, 40–43.

(26) Guo, Z.; Molesky, B. P.; Cheshire, T. P.; Moran, A. M. Elucidation of Reactive Wavepackets by Two-Dimensional Resonance Raman Spectroscopy. *J. Chem. Phys.* **2015**, *143*, 124202.

(27) Quick, M.; Dobryakov, A. L.; Kovalenko, S. A.; Ernsting, N. P. Resonance Femtosecond-Stimulated Raman Spectroscopy without Actinic Excitation Showing Low-Frequency Vibrational Activity in the S2 State of All-Trans β -Carotene. *J. Phys. Chem. Lett.* **2015**, *6*, 1216–1220.

(28) Fumero, G.; Batignani, G.; Dorfman, K. E.; Mukamel, S.; Scopigno, T. On the Resolution Limit of Femtosecond Stimulated Raman Spectroscopy: Modelling Fifth-Order Signals with Overlapping Pulses. *ChemPhysChem* **2015**, *16*, 3438–3443.

(29) Harel, E.; Fidler, A. F.; Engel, G. S. Single-Shot Gradient-Assisted Photon Echo Electronic Spectroscopy. *J. Phys. Chem. A* **2011**, *115*, 3787–3796.

(30) Spokoiny, B.; Harel, E. Mapping the Vibronic Structure of a Molecule by Few-Cycle Continuum Two-Dimensional Spectroscopy in a Single Pulse. *J. Phys. Chem. Lett.* **2014**, *5*, 2808–2814.

(31) Chachisvilis, M.; Fidler, H.; Pullerits, T.; Sundström, V. Coherent Nuclear Motions in Light-Harvesting Pigments and Dye Molecules, Probed by Ultrafast Spectroscopy. *J. Raman Spectrosc.* **1995**, *26*, 513–522.

(32) Selig, U.; Langhojer, F.; Dimler, F.; Löhrig, T.; Schwarz, C.; Giesekeing, B.; Brixner, T. Inherently Phase-Stable Coherent Two-Dimensional Spectroscopy Using Only Conventional Optics. *Opt. Lett.* **2008**, *33*, 2851–2853.

(33) Molesky, B. P.; Giokas, P. G.; Guo, Z.; Moran, A. M. Multidimensional resonance raman spectroscopy by six-wave mixing in the deep UV. *J. Chem. Phys.* **2014**, *141*, 114202.

(34) Garrett-Roe, S.; Hamm, P. Purely absorptive three-dimensional infrared spectroscopy. *J. Chem. Phys.* **2009**, *130*, 164510.